

Published in final edited form as:

Bioorg Med Chem Lett. 2012 September 1; 22(17): 5685–5688. doi:10.1016/j.bmcl.2012.06.098.

Optimization of tricyclic Nec-3 necroptosis inhibitors for *in vitro* liver microsomal stability

Sungwoon Choi^{a,e}, Heather Keys^b, Richard J. Staples^c, Junying Yuan^d, Alexei Degterev^b, and Gregory D. Cuny^{a,f,*}

^aLaboratory for Drug Discovery in Neurodegeneration, Harvard NeuroDiscovery Center, Brigham & Women's Hospital and Harvard Medical School, 65 Landsdowne Street, Cambridge, MA 02139, USA

^bDepartment of Biochemistry, Tufts University Medical School, 136 Harrison Avenue, Stearns 703, Boston, MA 02111, USA

^cDepartment of Chemistry, Michigan State University, 578 S. Shaw Lane, East Lansing, MI 48824, USA

^dDepartment of Cell Biology, Harvard Medical School, 240 Longwood Avenue, Boston, MA 02115, USA

^eDepartment of Scientific Criminal Investigation, Chungnam National University, Daejeon, 305-764, Korea

^fDepartment of Pharmacological and Pharmaceutical Sciences, University of Houston, College of Pharmacy, 549A Science and Research Bldg 2, Houston, TX 77204, USA

Abstract

Necroptosis is a regulated caspase-independent cell death pathway with morphological features resembling passive non-regulated necrosis. Several diverse structure classes of necroptosis inhibitors have been reported to date, including a series of 3,3a,4,5-tetrahydro-2H-benz[g]indazoles (referred to as the Nec-3 series) displaying potent activity in cellular assays. However, evaluation of the tricyclic necroptosis inhibitor's stability in mouse liver microsomes indicated that they were rapidly degraded. A structure-activity relationship (SAR) study of this compound series revealed that increased liver microsomal stability could be accomplished by modification of the pendent phenyl ring and by introduction of a hydrophilic substituent (i.e. α -hydroxyl) to the acetamide at the 2-position of the tricyclic ring without significantly compromising necroptosis inhibitory activity. Further increases in microsomal stability could be achieved by utilizing the 5,5-dioxo-3-phenyl-2,3,3a,4-tetrahydro-[1]benzothiopyrano[4,3-c]pyrazoles. However, in this case necroptosis inhibitory activity was not maintained. Overall, these results provide a strategy for generating potent and metabolically stable tricyclic necrostatin analogs (e.g. **33**, LDN-193191) potentially suitable for *in vivo* studies.

Necroptosis is a regulated caspase-independent cell death pathway with morphological features resembling passive non-regulated necrosis.^{1,2} This type of cell death can be

© 2012 Elsevier Ltd. All rights reserved.

*To whom correspondence should be addressed: Phone: +1-713-743-1274, Fax: +1-713-743-1884, gdcuny@central.uh.edu.

Publisher's Disclaimer: This is a PDF file of an unedited manuscript that has been accepted for publication. As a service to our customers we are providing this early version of the manuscript. The manuscript will undergo copyediting, typesetting, and review of the resulting proof before it is published in its final citable form. Please note that during the production process errors may be discovered which could affect the content, and all legal disclaimers that apply to the journal pertain.

initiated with various stimuli (e.g. TNF- α and Fas ligand) and in a variety of cell types (e.g. monocytes, fibroblasts, lymphocytes, macrophages, epithelial cells and neurons). Furthermore, necroptosis may represent a significant contributor to and in some cases predominant mode of cellular demise under pathological conditions involving excessive cell stress, rapid energy loss and massive oxidative species generation, not conducive for highly energy-dependent processes, such as apoptosis. Regulated necrotic cell death mechanisms, such as necroptosis, raises the possibility of novel therapeutic intervention strategies for the treatment of conditions where necrosis is known to play a prominent role, such as organ ischemia (i.e. stroke³ and myocardial infarction⁴), trauma and possibly some forms of neurodegeneration.⁵

To date several diverse structure classes of necroptosis inhibitors have been reported, including hydantoin containing indole derivatives (i.e. **1**),⁶ rel-(3*R*,3*aR*)-3-phenyl-3,3*a*,4,5-tetrahydro-2*H*-benz[*g*]indazoles (i.e. **2**),⁷ substituted 3*H*-thieno[2,3-*d*]pyrimidin-4-ones (i.e. **3**),⁸ [1,2,3]thiadiazole benzylamides (i.e. **4**)⁹ and pyrrole benzylamides (i.e. **5**)¹⁰ (Figure 1). Many of these compounds block necroptosis through inhibition of receptor interacting protein 1 (RIP1) kinase.¹¹ In addition, (\pm)-**1** has demonstrated *in vivo* activity in the temporary and permanent middle cerebral artery occlusion (MCAO) model of cerebral ischemia¹, in a mouse model of ischemia/reperfusion heart injury,¹² in the controlled cortical impact (CCI) model of traumatic brain injury (TBI),¹³ a retinal ischemia-reperfusion injury model,¹⁴ a systemic inflammatory response syndrome (SIRS) model,¹⁵ and a Huntington's disease model.¹⁶

In order to evaluate the *in vivo* pharmacology of other necroptosis inhibitors via preferred administration routes (i.e. oral, intravenous, intraperitoneal or subcutaneous) they must possess adequate metabolic stability, in addition to *in vitro* potency. One efficient and cost effective method of assessing a compound's metabolic stability is to measure its resistance to metabolism over time in the presence of liver microsomes.¹⁷ Utilizing this technique with mouse liver microsomes, compound **2**, which inhibits necroptosis induced with TNF- α in FADD-deficient variant of human Jurkat T cells with an EC₅₀ value of 0.29 μ M, demonstrated poor metabolic stability with a half-life ($t_{1/2}$) of 8.2 min and intrinsic clearance (CL_{int}) of 169 \pm 2.0 μ L/min/mg protein. Herein, we describe the results of a SAR study to optimize the *in vitro* liver microsomal stability of the tricyclic (Nec-3) class of necroptosis inhibitors.

Many of the tricyclic derivatives evaluated herein were prepared according to the procedure outlined in Scheme 1.⁷ 1-Tetralones, 4-chromanones and 4-thiochromanones, **6**, were treated with benzaldehydes or phenylacetaldehyde under basic or acid conditions to give **7**. The chalcones were allowed to react with hydrazine hydrate utilizing various acids (R³CO₂H) as solvent to give a mixture of two diastereomers, the (3*R*,3*aR*)-rel-isomers **8a** – **11a** and the (3*R*,3*aS*)-rel-isomers **8b** – **11b**. The diastereomers were readily separated by column chromatography on silica gel and the stereochemical assignments were made using ¹H-NMR. Removal of the benzyl group in **9a** was accomplished by hydrogenation in the presence of 10% Pd/C to give alcohol **12**. Oxidation of **10a** and **11a** with *m*-chloroperoxybenzoic acid (*m*-CPBA) gave sulfones **13** and **14**, respectively. Sulfone **14** was subsequently converted to alcohol **15** by hydrogenation.

Derivatives containing a methyl group at the 3*a*-position were prepared according to the procedure outlined in Scheme 2. Initial attempts to prepare these derivatives from an α -methyl-1-tetralone derivative utilizing the same synthetic strategy employed for the preparation of the 3*a*-H derivatives were unsuccessful. Instead, 7-methoxy-1-tetralone, **16**, was deprotonated with NaN(TMS)₂ and then allowed to react with 4-methoxybenzoyl chloride to give the 1,3-diketone **17**. This compound was again subjected to the same

process, except that the anion was quenched with iodomethane to give 1,3-diketone **18**. Condensation of **18** with hydrazine hydrate in the presence of 4Å molecular sieves gave **19**.¹⁸ Treatment of **19** at -78 °C with acetyl chloride followed by reduction of the *in situ* generated acyl iminium gave a mixture of diastereomers **20a** and **20b** in a ratio of 1:1.7, favoring isomer **20b** where the hydride anion approaches the acyl iminium intermediate distal to the 3a-Me. The 3a-Me of **20b**, which is *syn* to the pendent phenyl, was shielded and appeared at δ 0.69 in the ¹H NMR spectra.^{19a} The 3a-Me of **20a** appeared further downfield at δ 1.59.^{19b} The structure of **20b** was confirmed by single crystal x-ray analysis and reaffirmed the regioselectivity of the acylation reaction and the stereochemical assignments of the diastereomers (Figure 2).²⁰

In vitro microsomal stability was determined in pooled mouse liver microsomes. Test compounds (Table 1) were incubated in the presence and absence of NADPH for 0 – 60 min and the amount of remaining compound was quantified.²¹ Necroptosis inhibitor (\pm)-**1** demonstrated good metabolic stability in this assay with a $t_{1/2}$ = 59.1 min and CL_{int} = 23.5 ± 2.1 μ L/min/mg protein. Evaluation of necroptosis inhibitory activity was performed using a FADD-deficient variant of human Jurkat T cells treated with TNF- α as previously described.^{1, 7} Utilizing these conditions the cells efficiently underwent necroptosis, which was completely and selectively inhibited by (\pm)-**1** (EC_{50} = 0.21 μ M). For EC_{50} value determinations, cells were treated with 10 ng/mL of human TNF- α in the presence of increasing concentration of test compounds (eleven doses between 30 nM to 100 μ M) for 24 h followed by ATP-based viability assessment.

Several regions of the tricyclic necroptosis inhibitor **2** were considered potential liability sites responsible for the compound's poor metabolic stability in mouse liver microsomes. These sites included the methoxy groups at both the 8-position of the tricyclic ring and the 4-position of the pendent phenyl, the dihydropyrazole ring, the benzylic carbon at the 5-positions and the amide at the 2-position.

Introduction of a methyl group at the 3a-position of the tricyclic ring (**20a** and **20b**), which was envisioned to block potential oxidation of the dihydropyrazole, did not result in improved stability. Interestingly, necroptosis inhibitory activity was dramatically decreased for both diastereomers. Replacement of the benzylic methylene at the 5-position with oxygen (**22**) did not result in an increase in metabolic stability. When the methoxy group at the 8-position of the tricyclic ring was further replaced with a fluorine (**23**) metabolic stability remained poor. Substitution of the benzylic methylene with sulfur (**24**) similarly did not improve stability. However, replacement with a sulfone (**25**) did result in a significant increase in metabolic stability ($t_{1/2}$ = 40 min and CL_{int} = 34.6 ± 2.6 μ L/min/mg protein) with a slight decrease in necroptosis inhibitory activity. Introduction of a methylene group between the 3-position of the tricyclic ring and the pendent phenyl ring (**26**) similarly did not increase stability, but did eliminate necroptosis inhibitory activity. Addition of a hydroxyl group on the α -position of the amide (**27** vs. **2** and **28** vs. **29**) or introduction of a trifluoromethoxy in place of a methoxy at the 4-position of the pendent phenyl ring (**30** vs. **2**) resulted in increased metabolic stability. A combination of these changes (**31**) yielded a further increase in stability ($t_{1/2}$ = 54 min and CL_{int} = 25.5 ± 3.8 μ L/min/mg protein). A similar result was also found with a sulfone derivative (**25** vs. **32**), albeit necroptosis inhibitory activity was compromised. Although introduction of fluorine at the 3-position of the pendent phenyl ring did not increase stability in one case (**2** vs. **28**), in another instance this change in combination with a hydroxyl group on the α -position of the amide and a trifluoromethoxy at the 4-position of the pendent phenyl (**2** vs. **33**) resulted in a significant (18-times) stability increase ($t_{1/2}$ = 148 min and CL_{int} = 9.38 ± 1.4 μ L/min/mg protein) with only a modest (2-fold) decrease in necroptosis inhibitory activity.

In conclusion, increased liver microsomal stability as well as improvement in activity were accomplished for the tricyclic (Nec-3) series of necroptosis inhibitors by modification of the pendent phenyl and by introduction of a hydrophilic substituent (i.e. α -hydroxyl) to the acetamide at the 2-position, resulting in inhibitor **33** (LDN-193191).^{19c} The benzylic position of the tricyclic ring also appeared to influence metabolic stability. Although replacement of the methylene group with a sulfone increased metabolic stability, it significantly decreased necroptosis inhibitory activity. Additional optimization of tricyclic necroptosis inhibitors utilizing the information from this study may result in further increases in metabolic stability and provide a unique set of necroptosis inhibitors suitable for *in vivo* analysis of the pathologic role of necroptosis following acute and potentially chronic injury.

Acknowledgments

SC and GDC thank the Harvard NeuroDiscovery Center (HNC) for financial support. AD and JY thank the National Institute on Aging, National Institute of General Medical Sciences and American Health Assistance Foundation for financial support. SC, GDC and JY thank the National Institute of Neurological Disorders and Stroke (NINDS) for financial support. AD is a recipient of NIH Mentored Scientist Development Award from the National Institute on Aging (NIA).

References and Notes

- Degterev A, Huang Z, Boyce M, Li Y, Jagtap P, Mizushima N, Cuny GD, Mitchison T, Moskowitz M, Yuan J. *Nat Chem Biol.* 2005; 1:112. [PubMed: 16408008]
- For review articles related to necroptosis see: Yuan J, Kroemer G. *Genes Dev.* 2010; 24:2592. [PubMed: 21123646] Vandenabeele P, Galluzzi L, Vanden Berghe T, Kroemer G. *Nat Rev Mol Cell Biol.* 2010; 11:700. [PubMed: 20823910] Christofferson DE, Yuan J. *Curr Opin Cell Biol.* 2010; 22:263. [PubMed: 20045303] Degterev A, Yuan J. *Nat Rev Mol Cell Biol.* 2008; 9:378. [PubMed: 18414491]
- (a) Mehta SL, Manhas N, Raghubir R. *Brain Res Rev.* 2007; 54:34. [PubMed: 17222914] (b) Lo EH, Dalkara T, Moskowitz MA. *Nat Rev Neurosci.* 2003; 4:399. [PubMed: 12728267]
- (a) Whelan RS, Kaplinskiy V, Kitsis RN. *Annu Rev Physiol.* 2010; 72:19. [PubMed: 20148665] (b) McCully JD, Wakiyama H, Hsieh YJ, Jones M, Levitsky S. *Am J Physiol Heart Circ Physiol.* 2004; 286:H1923. [PubMed: 14715509]
- (a) Esposito E, Cuzzocrea S. *Curr Med Chem.* 2010; 17:2764. [PubMed: 20586718] (b) Martin LJ, Al-Abdulla NA, Brambrink AM, Kirsch JR, Sieber FE, Portera-Cailliau C. *Brain Res Bull.* 1998; 46:281. [PubMed: 9671259]
- Teng X, Degterev A, Jagtap P, Xing X, Choi S, Denu R, Yuan J, Cuny GD. *Bioorg Med Chem Lett.* 2005; 15:5039. [PubMed: 16153840]
- Jagtap PG, Degterev A, Choi S, Keys H, Yuan J, Cuny GD. *J Med Chem.* 2007; 50:1886. [PubMed: 17361994]
- Wang K, Li J, Degterev A, Hsu E, Yuan J, Yuan C. *Bioorg Med Chem Lett.* 2007; 17:1455. [PubMed: 17270434]
- Teng X, Keys H, Jeevanandam A, Porco JA Jr, Degterev A, Yuan J, Cuny GD. *Bioorg Med Chem Lett.* 2007; 17:6836. [PubMed: 17964153]
- Teng X, Keys H, Yuan J, Degterev A, Cuny GD. *Bioorg Med Chem Lett.* 2008; 18:3219. [PubMed: 18467094]
- Degterev A, Hitomi J, Gernsheid M, Ch'en I, Korkina O, Teng X, Abbott D, Cuny GD, Yuan C, Wagner G, Hedrick SM, Gerber SA, Lugovskoy A, Yuan J. *Nat Chem Biol.* 2008; 4:313. [PubMed: 18408713]
- Smith CCT, Davidson SM, Lim SY, Simpkin JC, Hothersall JS, Yellon DM. *Cardiovasc Drugs Ther.* 2007; 21:227. [PubMed: 17665295]
- You Z, Savitz SI, Yang J, Degterev A, Yuan J, Cuny GD, Moskowitz MA, Whalen MJ. *J Cereb Blood Flow Metab.* 2008; 28:1564. [PubMed: 18493258]

14. Rosenbaum DM, Degterev A, David J, Rosenbaum PS, Roth S, Grotta JC, Cuny GD, Yuan J, Savitz SI. *J Neurosci Res.* 2010; 88:1569. [PubMed: 20025059]
15. Duprez L, Takahashi N, Van Hauwermeiren F, Vandendriessche B, Goossens V, Vanden Berghe T, Declercq W, Libert C, Cauwels A, Vandenabeele P. *Immunity.* 2011; 35:908. [PubMed: 22195746]
16. Zhu S, Zhang Y, Bai G, Li H. *Cell Death Dis.* 2011; 2:e115. [PubMed: 21359116]
17. Baranczewski P, Staczak A, Sundberg K, Svensson R, Wallin A, Jansson J, Garberg P, Postlind H. *Pharmacol Rep.* 2006; 58:453. [PubMed: 16963792]
18. Adam W, Librera CP. *J Org Chem.* 2002; 67:576. [PubMed: 11798332]
19. (a) ^1H NMR of **20a** (500 MHz, CDCl_3): δ 1.59 (s, 3H), 1.78–1.82 (m, 2H), 2.35 (s, 3H), 2.35–2.45 (m, 2H), 3.78 (s, 3H), 3.85 (s, 3H), 5.39 (s, 1H), 6.74 (dd, $J_1 = 8.5$ Hz, $J_2 = 3.0$ Hz, 1H), 6.92–6.95 (m, 3H), 7.51 (d, $J = 3.0$ Hz, 1H), 7.70 (d, $J = 8.5$ Hz, 2H). (b) ^1H NMR of **20b** (500 MHz, CDCl_3): δ 0.69 (s, 3H), 2.05–2.14 (m, 2H), 2.46 (s, 3H), 2.85–3.01 (m, 2H), 3.80 (s, 3H), 3.86 (s, 3H), 4.93 (s, 1H), 6.88 (d, $J = 9.0$ Hz, 1H), 6.92 (dd, $J_1 = 9.0$ Hz, $J_2 = 2.5$ Hz, 1H), 7.10–7.12 (m, 3H), 7.41 (d, $J = 2.5$ Hz, 1H). (c) ^1H NMR of **33** (500 MHz, CDCl_3): δ 1.01–1.10 (m, 1H), 1.79–1.84 (m, 1H), 2.81–2.88 (m, 2H), 3.58–3.64 (m, 1H), 3.88 (s, 3H), 4.59–4.74 (m, 2H), 5.69 (d, $J = 11.0$ Hz, 1H), 6.89–6.97 (m, 3H), 7.09 (d, $J = 8.5$ Hz, 1H), 7.24–7.28 (m, 1H), 7.48 (d, $J = 2.5$ Hz, 1H).
20. CCDC 875792 contains the supplementary crystallographic data for this paper. These data can be obtained free of charge from The Cambridge Crystallographic Data Centre via www.ccdc.cam.ac.uk/data_request/cif.
21. Microsomal stability was determined in pooled mouse liver microsomes. Test compound (3 μM final concentration) along with 0.5 mg/mL microsome protein and 1 mM NADPH was incubated for 0, 5, 15, 30 and 60 min. Incubation of test compound and microsomes in the absence of NADPH served as a negative control. The samples were quenched with methanol and centrifuged for 20 min at 2500 rpm to precipitate proteins. Sample supernatants were analyzed (N=3) by LC/MS. The \ln peak area ratio (compound peak area/internal standard peak area) was plotted against time and the slope of the line determined to give the elimination rate constant [$k = (-1)(\text{slope})$]. The half life ($t_{1/2}$ in minutes), and the *in vitro* intrinsic clearance (CL_{int} in $\mu\text{L}/\text{min}/\text{mg}$ protein) were calculated according to the following equations, where V = incubation volume in $\mu\text{L}/\text{mg}$ protein:

$$t_{1/2} = \frac{0.693}{k}; CL_{\text{int}} = \frac{V(0.693)}{t_{1/2}}.$$

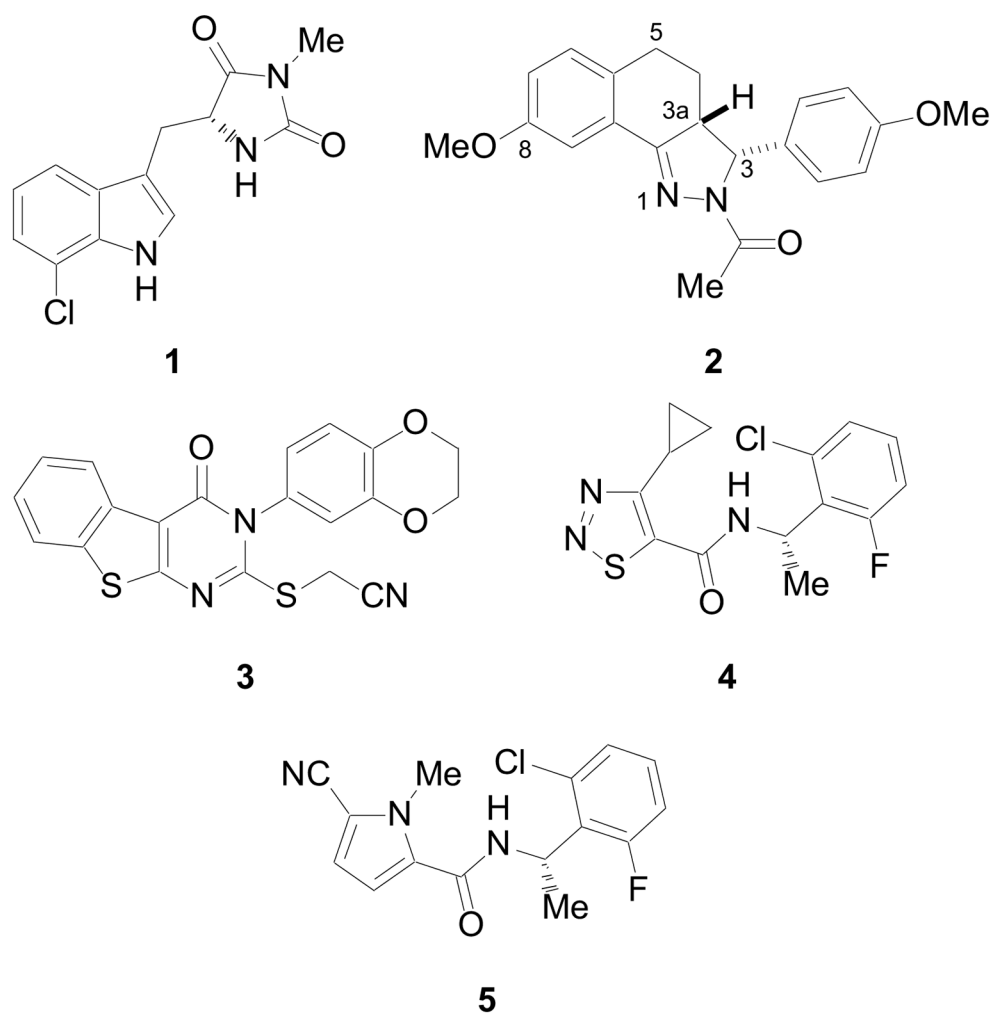


Figure 1.
Necrostatins. The numbering convention of **2** is also shown.

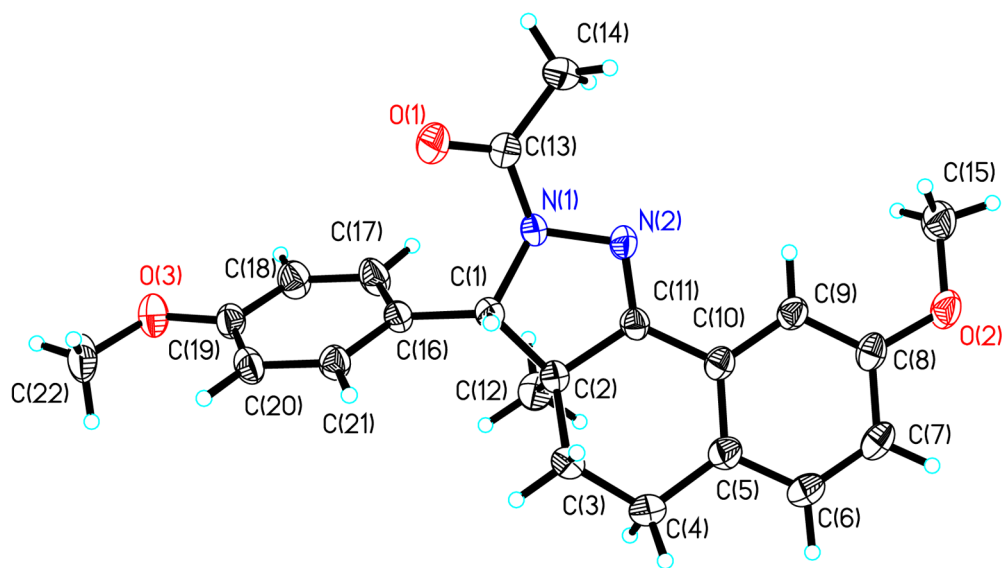
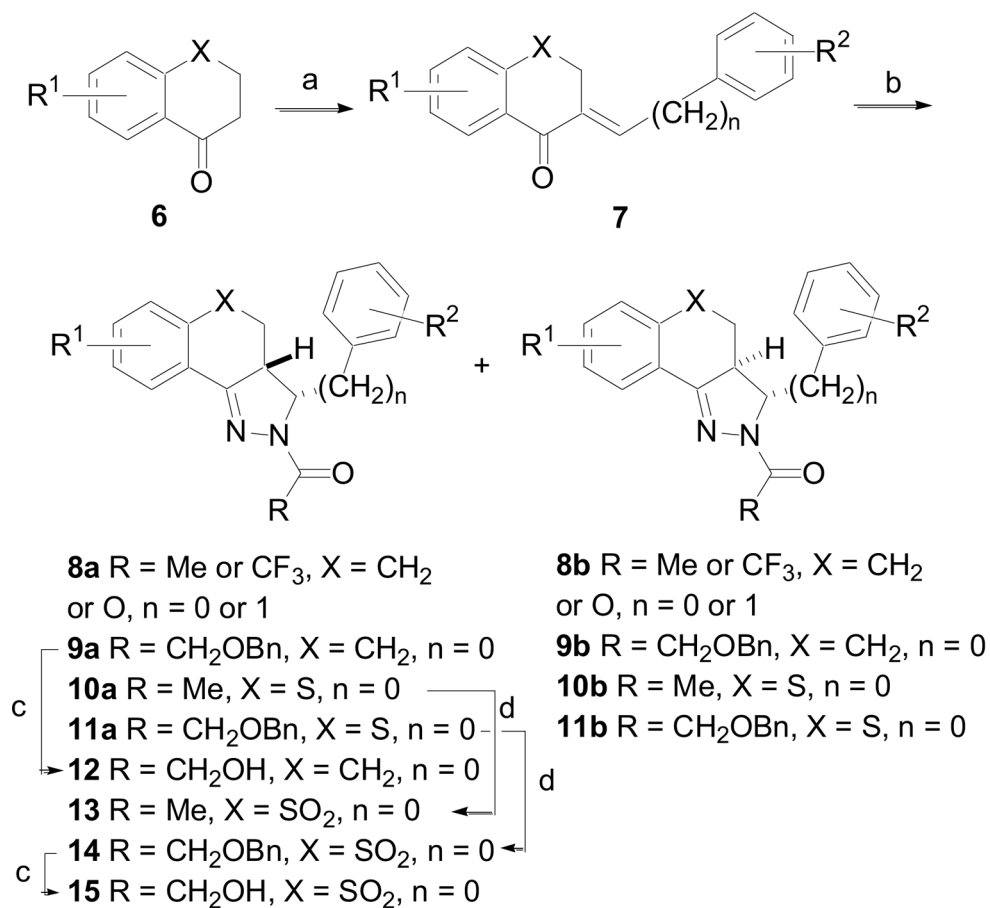
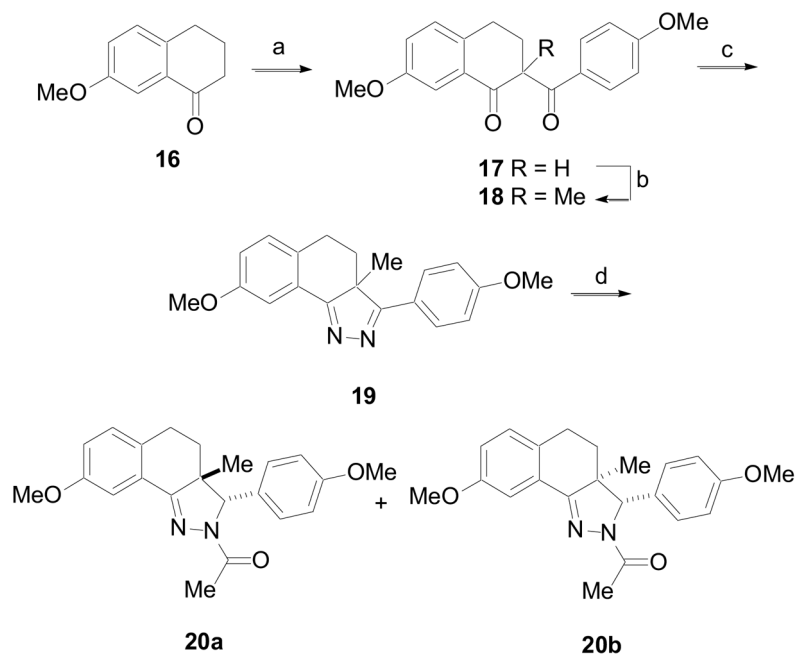


Figure 2.
Thermal ellipsoidal drawing of **20b** as determined by single crystal x-ray analysis.

**Scheme 1.**

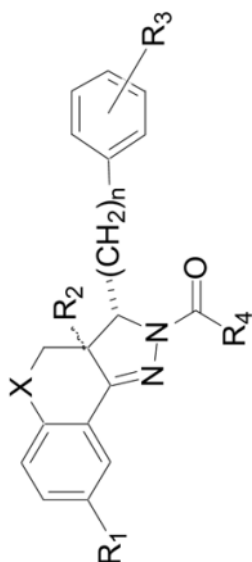
(a) Ar(CH₂)_nCHO, 8N NaOH, EtOH, rt, 2 h or Ar(CH₂)_nCHO, conc HCl, MeOH, Δ, 4 h (60 – 75%); (b) R³CO₂H, NH₂NH₂·xH₂O, 120 °C, 15 h (70 – 80% when n = 0; 20% when n = 1); (c) H₂ (1 atm), 10% Pd/C, EtOH (47–75%); (d) MCPBA, DCM, rt, 16 h (90–96%).

**Scheme 2.**

(a) $\text{NaN}(\text{TMS})_2$, THF, 0 °C, then 4-MeO-PhC(O)Cl, 0 °C to rt (80%); (b) $\text{NaN}(\text{TMS})_2$, THF, 0 °C, then MeI, 0 °C to rt (91%); (c) $\text{NH}_2\text{NH}_2 \cdot x\text{H}_2\text{O}$, DCM, 4 Å molecular sieves (52%); (d) $\text{MeC}(\text{O})\text{Cl}$, DCM, -78 °C, then $\text{NaBH}(\text{OAc})_3$, -78 °C to rt (95%).

Table 1

Compounds prepared for microsomal stability studies and EC₅₀ determinations for necroptosis inhibition in FADD-deficient Jurkat T cells treated with TNF- α .



| Compound | R ¹ | R ² | R ³ | R ⁴ | X | n |
|----------|----------------|-------------------------|-------------------------|--------------------|-----------------|---|
| 2 | OMe | β -H ^a | 4-OMe | Me | CH ₂ | 0 |
| 20a | OMe | β -Me | 4-OMe | Me | CH ₂ | 0 |
| 20b | OMe | α -Me | 4-OMe | Me | CH ₂ | 0 |
| 21 | OMe | β -H | 4-OMe | CF ₃ | CH ₂ | 0 |
| 22 | OMe | β -H | 4-OMe | Me | O | 0 |
| 23 | F | β -H | 4-OMe | Me | O | 0 |
| 24 | OMe | β -H | 4-OMe | Me | S | 0 |
| 25 | OMe | β -H | 4-OMe | Me | SO ₂ | 0 |
| 26 | OMe | β -H | H | Me | CH ₂ | 1 |
| 27 | OMe | β -H | 4-OMe | CH ₂ OH | CH ₂ | 0 |
| 28 | OMe | β -H | 3-F, 4-OMe | Me | CH ₂ | 0 |
| 29 | OMe | β -H | 3-F, 4-OMe | CH ₂ OH | CH ₂ | 0 |
| 30 | OMe | β -H | 4-OCF ₃ | Me | CH ₂ | 0 |
| 31 | OMe | β -H | 4-OCF ₃ | CH ₂ OH | CH ₂ | 0 |
| 32 | OMe | β -H | 4-OCF ₃ | CH ₂ OH | SO ₂ | 0 |
| 33 | OMe | β -H | 3-F, 4-OCF ₃ | CH ₂ OH | CH ₂ | 0 |

^a α -H refers to the (3*R*,3*a*,*S*)-rel-diastereomer; β -H refers to the (3*R*,3*a*,*R*)-rel-diastereomer.

Table 2

EC₅₀ determinations for necroptosis inhibition in FADD-deficient Jurkat T cells treated with TNF- α and mouse microsomal stability values.

| Compound | EC ₅₀ (μ M) ^a | t _{1/2} (min) | CL _{int} (μ L/min/mg protein) |
|------------|--|------------------------|---|
| 2 | 0.29 | 8.2 | 169 \pm 2.0 |
| 20a | > 100 | 2.9 | 476 \pm 53.9 |
| 20b | 15 | 7.2 | 194 \pm 5.9 |
| 21 | 0.39 | 15 | 90.7 \pm 13.4 |
| 22 | 0.46 | 10 | 135 \pm 9.3 |
| 23 | 12 | 11 | 120 \pm 39.3 |
| 24 | 0.28 | 12 | 115 \pm 18.5 |
| 25 | 0.75 | 40 | 34.6 \pm 2.6 |
| 26 | > 100 | 3.0 | 463 \pm 78.1 |
| 27 | 0.16 | 33 | 42.4 \pm 5.5 |
| 28 | 0.090 | 8.6 | 162 \pm 5.7 |
| 29 | 0.28 | 27 | 50.5 \pm 3.6 |
| 30 | 0.33 | 20 | 68.7 \pm 18.0 |
| 31 | 0.64 | 54 | 25.5 \pm 3.8 |
| 32 | 27 | 115 | 12.1 \pm 1.4 |
| 33 | 0.61 | 148 | 9.38 \pm 1.4 |

^aStandard deviation < 10%.